Available online at www.sciencedirect.com

ScienceDirect

IFAC Papers Online CONFERENCE PAPER ARCHIVE

IFAC PapersOnLine 50-1 (2017) 3680–3684

Autonomous Landing of UAVs under Unknown Disturbances using NDI Autopilot with L_1 Adaptive Augmentation

Amit K Tripathi * **Vijay V Patel** ** **Radhakant Padhi** ***

* *Scientist, Aeronautical Development Agency, Bangalore, India.*
** *Scientist, Aeronautical Development Agency, Bangalore, India.*
*** *Professor, Indian Institute of Science, Bangalore, India. (E-mail: padhi@aero.iisc.ernet.in)*

Abstract: This paper presents autonomous landing of Unmanned Aerial Vehicles (UAVs) under unknown external disturbances and internal plant parameter uncertainties. The external disturbances such as wind shear, wind gust and ground effects are considered. The plant parameters uncertainties are also considered due to aerodynamic force and moment coefficients random perturbation. L_1 adaptive controller with piece-wise-constant adaptation law is augmented over Nonlinear Dynamic Inversion (NDI) autopilot and implemented on Six Degree of Freedom (Six-DOF) model of a UAV. The NDI autopilot with two time scale separation is designed for the nominal plant. It tracks a reference trajectory computed from a path planning and guidance algorithm under undisturbed plant model with normal environment conditions. The L_1 adaptive controller takes into account the disturbances and computes the adaptive control command which enables the plant trajectory tracking closer to the desired reference trajectory. The state predictor is designed to track the plant states smoothly by incorporating proportional and integral error terms in the state predictor model. The piece-wise-constant adaptive law is designed to estimate the unknown disturbances. The unknown disturbance estimates are used to design the adaptive control law to nullify the effect of the disturbance on the plant performance. The algorithm is simulated to show the auto landing performance on a Six-DOF UAV model.

Keywords: L_1 Adaptive, piece-wise-constant, state predictor, dynamic-inversion, Six-DOF, autolanding, glideslope, flare, tracking

1. INTRODUCTION

The autonomous landing plays a very important role for UAVs. The landing phase of flight is considered as one of the most critical phase as it requires precision and smoothness and minimum delay. During landing, the UAV may be severely affected by the external disturbances such as crosswinds, wind shear, wind gusts and the ground effects. Most UAVs accidents occurred due to low level wind shear while they attempt to take off and land Frost and Bowles (1984). Ground effect during landing causes induced lift and reduced drag due to which the sink rate of UAV is reduced and it takes long runway to touchdown.

In the literature many control strategies are developed for auto-landing. Nonlinear controllers such as NDI Singh and Padhi (2009) can be used for auto landing however it has the problem of singularity as well as it requires the full state of the system. The NDI autopilot does not account for the unknown disturbances and its robustness performance is poor. The other control strategies are Feedback linearization controller Prasad and Pradeep (2007); Wagner and Valasek (2007) are also used for auto landing problem but they also have linearization and gain scheduling limitations.

Adaptive control techniques are very effective to deal with uncertainties and parameter variations in the system dynamics. The philosophy of the L_1 adaptive state feedback controller for unmatched uncertainties Hovakimyan and Cao (2010) is to obtain an estimate of the uncertainties and define a control signal which compensates for the effect of these uncertainties on the output within the bandwidth of low-pass filters introduced in the feedback loop. These filters guarantee that the L_1 adaptive controller stays in the low-frequency range even in the presence of fast adaptation and large reference inputs. Adaptation is based on a piecewise constant adaptive law Peter et al. (2012) and uses the output of a state predictor to update the estimate of the uncertainties.

The path planning and guidance is designed for autonomous landing. The autonomous landing comprise of mainly three phases Prasad and Pradeep (2007) such as alignment and approach phase, where UAV aligns with the runway by correcting the heading. Next is glideslope phase, where the UAV follows a fixed ramp path with constant flight path angle until it reaches a flare height. During the glideslope phase UAV descends with a higher sink rate. Once the flare height is achieved the UAV follows a exponential trajectory until the touchdown point. Flare is an important phase of UAV and the altitude control should be very efficient as well as ground effects are also dominant in this phase due to proximity with ground. The different phases of autolanding is shown in Fig. 1.

L_1 adaptive controller compensates for the uncertainty within the the bandwidth of the low pass filter. The significant benefit of L_1 adaptive control architecture is that it does not invert

2405-8963
Peer review under responsibility of International Federation of Automatic Control.
10.1016/j.ifacol.2017.08.561

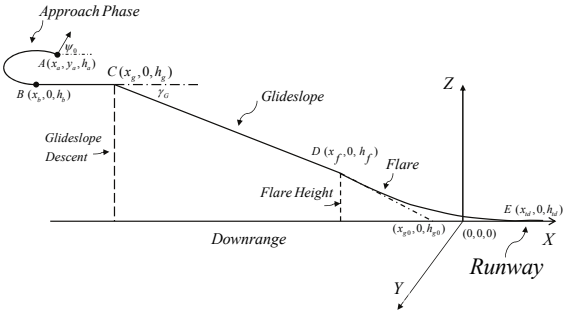

Fig. 1. Auto-landing Phases of an Unmanned Ariel Vehicle

the system dynamics. L_1 adaptive controller simultaneously computes the actual plant dynamics and predictor dynamics and computes the error between the states of the two dynamics. This error is fed to the piece wise constant adaptive law which computes the estimated parameter uncertainty. This estimated parameter uncertainty is used to compute the L_1 adaptive controller commands.

2. MATHEMATICAL MODEL OF UAV

Simulations require an accurate and realistic mathematical model of the dynamical system under nominal and perturbed conditions. The nominal Six-DOF model as well as Six-DOF model with wind disturbances and ground effect are described in this section for AE-2 UAV.

2.1 Nonlinear UAV State Dynamics

Assuming the UAV to be a rigid body and earth to be flat the complete set of Six-DOF model equations are provided in Stevens et al. (2015); Anderson (2007).

Nominal Six-DOF Equations The Nominal Six-DOF equations for AE-2 model is provided as follows

$$\dot{U} = RV - QW - gsin\theta + X_a + X_t \tag{1}$$
$$\dot{V} = PW - RU + gsin\phi cos\theta + Y_a \tag{2}$$
$$\dot{W} = QU - PV + gcos\phi cos\theta + Z_a \tag{3}$$
$$\dot{P} = c_1 RQ + c_2 PQ + c_3 L_a + c_4 N_a \tag{4}$$
$$\dot{Q} = c_5 PR + c_6 (R^2 - P^2) + c_7 (M_a + M_t) \tag{5}$$
$$\dot{R} = c_8 PQ - c_2 RQ + c_4 L_a + c_9 N_a \tag{6}$$
$$\dot{\phi} = P + Qsin\phi tan\theta + Rcos\phi tan\theta \tag{7}$$
$$\dot{\theta} = Qcos\phi - Rsin\phi \tag{8}$$
$$\dot{\psi} = Qsin\phi sec\theta + Rcos\phi sec\theta \tag{9}$$
$$\dot{h} = Usin\theta - Vsin\phi cos\theta - Wcos\phi cos\theta \tag{10}$$

Where, coefficients $c_1 - c_9$ are functions of moment of inertia I_{xx}, I_{yy}, I_{zz} and I_{xz} as provided in Stevens et al. (2015). Nonlinear Six-DOF model is taken from data available in Chawla and Padhi (2011).

2.2 UAV Aerodynamic Model with Uncertainties

In this section, the UAV mathematical model with wind shear, wind gust and ground effect uncertainties will be described. The Six-DOF equations of motion with wind effects are derived by Etkin Etkin (2012) considering zero or constant wind.

Translational Kinematic Equations Wind Shear: Spatial and temporal variations of wind into Six-DOF model was proposed by Frost and Bowles (1984) as follows

$$\begin{bmatrix} \dot{x} \\ \dot{y} \\ \dot{h} \end{bmatrix} = \begin{bmatrix} U\cos\theta\cos\psi + V(\sin\phi\sin\theta\cos\psi - \cos\phi\sin\psi) \\ +W(\cos\phi\sin\theta\cos\psi + \sin\phi\sin\psi) + W_{xE} \\ U\cos\theta\sin\psi + V(\sin\phi\sin\theta\sin\psi + \cos\phi\cos\psi) \\ +W(\cos\phi\sin\theta\sin\psi - \sin\phi\cos\psi) + W_{yE} \\ U\sin\theta - V\sin\phi\cos\theta - W\cos\phi\cos\theta - W_{zE} \end{bmatrix} \tag{11}$$

Translational Dynamics with Wind Shear: Translational dynamics is affected by wind shear as well as wind shear rates. Time varying winds are most difficult to handle. In the literature, controllers are designed considering constant rate of change of wind shear Frost and Bowles (1984).

$$\begin{bmatrix} \dot{U} \\ \dot{V} \\ \dot{W} \end{bmatrix} = \begin{bmatrix} R(V + W_{yB}) - Q(W + W_{zB}) - \dot{W}_{xB} - g\sin\theta + \dfrac{X_a + X_t}{m} \\ P(W + W_{zB}) - R(U + W_{xB}) - \dot{W}_{yB} + g\sin\phi\cos\theta + \dfrac{Y_a}{m} \\ Q(U + W_{xB}) - P(V + W_{yB}) - \dot{W}_{zB} + g\cos\phi\cos\theta + \dfrac{Z_a}{m} \end{bmatrix} \tag{12}$$

3. NONLINEAR DYNAMIC INVERSION BASED GUIDANCE AND CONTROLLER DESIGN

Guidance design for glideslope and flare phases are described as follows

3.1 Glideslope Phase

The glideslope phase is shown in Fig. 1. The UAV follows a ramp path with constant slope which is given by flight path angle γ. The $(x_g, 0, h_g)$ is the point where the glide starts. The point $(0,0,0)$ shown in the figure is the origin of the inertial frame and it also shows the beginning of the runway. The point $(x_f, 0, h_f)$ shows the beginning of the flare and end of the glideslope. The point $(x_{g0}, 0, , h_{g0})$ which is nothing but the projection of the glideslope path to the ground. The typical reference γ is in the range $2.5^\circ - 3.5^\circ$. The desired slope of the path γ^* can be computed as

$$\gamma^* = \arctan\left(\frac{h_g - h_{g0}}{x_g - x_{g0}}\right) \tag{13}$$

we know that $h_{g0} = 0$. Therefore for any arbitrary point (x,h) on the glideslope path, the desired height h^* can be computed as

$$h^* = (x - x_{g0})\tan\gamma^* \tag{14}$$

3.2 Flare Phase

The flare phase of the landing is very critical phase due to its proximity with ground. The UAV descent rate is tightly controlled in this region. The trajectory of the flare considered in this paper is exponential. The desired height of the UAV is expressed as a function of downrange.

$$h^* = h_c + (h_f - h_c)e^{-k_x(x - x_f)} \tag{15}$$

The unknowns in the above equation are flare height h_f, distance at which to start flare x_f, height below ground where flare trajectory should end h_c and constant k_x. The four unknowns can be computed by imposing the following constraints on the Eq.(15).

Initial Condition The point where glideslope ends and flare begins should satisfy the constraints of both the trajectory. Therefore imposing that we obtain that,

$$h_f = -(x_f - x_{g0}) \tan \gamma^* \tag{16}$$

Initial Slope The slope of the glideslope should be same as the slope of the flare at the flare beginning point.

$$(h_f - h_c)k_x = \tan \gamma^* \tag{17}$$

Touchdown Condition At touchdown point $x = x_{td}$ the $h^* = 0$.

$$0 = h_c + (h_f - h_c)e^{-k_x(x_{td} - x_f)} \tag{18}$$

Sink Rate at Touchdown Condition The descent rate at touchdown should be equal to predefined sink rate.

$$\dot{h}_t^* = -(h_f - h_c)k_x \dot{x}_{td} e^{-k_x(x_{td} - x_f)} \tag{19}$$

The flight path angle can be computed with known sink rate at touchdown. Let the known sink rate is $\dot{h}_t^*$ then flight path angle γ at touchdown can be computed as $\gamma = \sin^{-1}(\dot{h}_t^*/V)$.

3.3 NDI Controller Design

Nonlinear Dynamic Inversion (NDI) controller is designed for a nonlinear dynamical system. The system should be affine in control. The UAV Six-DOF model has fast and slow state dynamics. Fast and slow state dynamics can be separated using time scale separation. The slower state dynamics uses fast states as control input and faster state dynamics uses actual control input.

$$\dot{X}_s = f_s(X) + g_s(X)X_f, \quad \dot{X}_f = f_f(X) + g_f(X)\nu_{bl}, \tag{20}$$

$$X = [X_s, X_f], \; X(0) = X_0, \; Y = h(X_s) \tag{21}$$

where, $X(t) \in \mathbb{R}^n$, $U(t) \in \mathbb{R}^m$ and $Y(t) \in \mathbb{R}^p$ are state, control and output vectors respectively of nonlinear dynamical system. The system is assumed to be point wise controllable. The objective is to design the baseline control ν_{bl} so that output Y tracks the commanded signal Y^* as $t \to \infty$. The Y^* is assumed to be bounded, smooth and slowly varying.

Using the chain rule of derivative, the expression for $\dot{Y}$ can be written as

$$\dot{Y} = f_Y(X) + g_Y(X)X_f \tag{22}$$

where, $f_Y(X) \triangleq \left[\frac{\partial h}{\partial X_s}\right] f_s(X)$ and $g_Y(X) \triangleq \left[\frac{\partial h}{\partial X_s}\right] g_s(X)$. Next, we define $E_1 \triangleq Y - Y^*$ and synthesize controller such that the first order error dynamics is satisfied.

$$\dot{E}_1 + K_1 E_1 = 0 \tag{23}$$

where, K_1 is a positive definite matrix. It can be chosen as diagonal matrix with positive elements. The elements represent the 'settling time constant'. Using the definition of E_1 and substituting the $\dot{Y}$ from Eq.(22) in Eq.(23), we can obtain the control expression after carrying out simple algebra

$$X_f{}^* = g_Y(X)^{-1}\left[-f_Y(X) - K_1(Y - Y^*) + \dot{Y}^*\right] \tag{24}$$

Similarly, one can obtain the obtain the following by imposing first order error dynamics with positive definite matrix K_2 and define error define $E_2 \triangleq X_f - X_f{}^*$

$$\nu_{bl} = \left[g_f(X)\right]^{-1}\left[-f_f(X) - K_2(X_f - X_f{}^*) + \dot{X}_f{}^*\right] \tag{25}$$

NDI contol technique provides close form solution without any computational difficulties. However, it requires an accurate knowledge of plant model. In the absence of accurate knowledge of plant model tracking will not be perfect and this difficulty can be addressed by augmenting NDI with L_1 adaptive controller. Fig.2 shows the over all auto landing architecture where NDI controller in two loop structure is the baseline controller and L_1 adaptive controller in two time separation loops augments the baseline NDI controller.

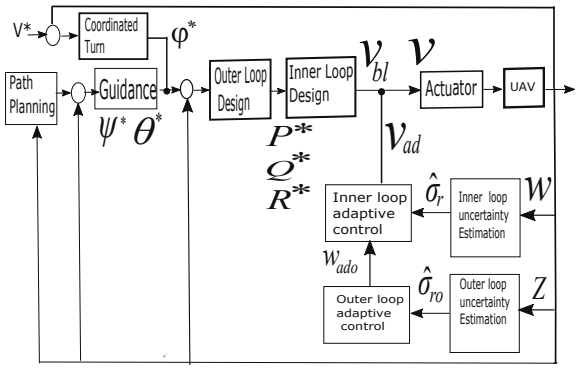

Fig. 2. Auto landing Architecture

4. L_1 ADAPTIVE CONTROLLER DESIGN

This section describes L_1 adaptive controller for a class of multi input multi output systems in the presence of uncertain system input gain and time and state dependent unknown nonlinearities, without enforcing matching conditions. The adaptive algorithm ensures uniformly bounded transient response for the systems signals, both input and output, simultaneously, in addition to steady state tracking.

L_1 adaptive controller is used where the system requires a better transient response, fast adaptation and robustness. L_1 adaptive controller does not use gain scheduling. It uses a prediction logic, adaptive gain logic and a low pass filter in controller command computation to eliminate high frequency signal content from controller output. The problem formulation using L_1 Adaptive control algorithm is presented in the following subsections.

4.1 Inner Loop L_1 Adaptive Control Design

L_1 Adaptive Augmentation for Inner Loop is designed as follows. The inner loop uncertainties are estimated and control laws are designed Peter et al. (2012) to nullify the effect of disturbances.

The Eq.(4) to Eq.(6) can be re written as

$$\dot{w}_r = \hat{A}_r(\wedge_r \nu_r + f_r) + \hat{B}_r \tag{26}$$

$$\hat{A}_r = \bar{q}S\begin{bmatrix} c_3 b & 0 & c_4 b \\ 0 & c_7 c & 0 \\ c_4 b & 0 & c_9 b \end{bmatrix}, \quad \wedge_r = \begin{bmatrix} C_{l_{\delta_a}} & 0 & 0 \\ 0 & C_{m_{\delta_e}} & 0 \\ 0 & 0 & C_{n_{\delta_r}} \end{bmatrix}, \nu_r = \begin{bmatrix} \delta_a \\ \delta_e \\ \delta_r \end{bmatrix}$$

$$f_r = \begin{bmatrix} C_{l_\beta}(\alpha)\beta + C_{l_p}(\alpha)\bar{P} + C_{l_r}(\alpha)\bar{R} \\ C_{m_0} + C_{m_\alpha}(\alpha)\alpha + C_{m_\beta}(\alpha,\beta)\beta + C_{m_q}(\alpha)\bar{Q} \\ C_{n_\beta}(\alpha)\beta + C_{n_p}(\alpha)\bar{P} + C_{n_r}(\alpha)\bar{R} \end{bmatrix}$$

and

$$\hat{B}_r = \begin{bmatrix} c_1RQ + c_2PQ \\ c_5PR + c_6(R^2 - P^2) + c_7M_t \\ c_8PQ - c_2RQ \end{bmatrix}$$

The terms are defined as $\hat{B}_r$ - Nominal nonlinearities of the dynamics, $\hat{A}_r$ - Approximate input matrix of the dynamics, $\wedge_r$ - Control effectiveness and f_r - Nonlinear term.

In order to design the inner loop state predictor, the plant dynamics in L_1 framework is provided as

$$\dot{w}_r = \hat{A}_r \nu_r + \hat{B}_r + \sigma_r, \quad \sigma_r = \hat{A}_r[(\wedge_r - I)\nu_r + f_r] \tag{27}$$

where σ_r is Composite Uncertainty and it estimates the uncertainties in the approximate model represented by $\hat{A}_r$ and $\hat{B}_r$.

Piece Wise Constant Adaptive Laws: Predictor equation for the inner loop state dynamics is given as

$$\dot{\hat{w}}_r = \hat{A}_r \nu_r + \hat{B}_r + \hat{\sigma}_r - K_{ep_{w_r}} \tilde{e}_{w_r} - K_{ep_{iw_r}} \tilde{e}_{iw_r} \tag{28}$$

$$\dot{\tilde{e}}_{iw_r} = \hat{e}_{w_r} - \hat{\sigma}_{\nu_r} \tag{29}$$

Where the prediction error terms are defined as

$$\tilde{e}_{w_r} = \hat{w}_r - w_r, \quad \tilde{e}_{iw_r} = \int [\hat{w}_r - w_r] dt \tag{30}$$

The prediction error dynamics is given as

$$\dot{\tilde{e}}_{w_r} = \hat{\sigma}_r - \sigma_r - K_{ep_{w_r}} \tilde{e}_{w_r} - K_{ep_{iw_r}} \tilde{e}_{iw_r} \tag{31}$$

Error Dynamics: Error Dynamics for inner loop L_1 adaptive control is provided as

$$\begin{bmatrix} \dot{\tilde{e}}_{iw_r} \\ \dot{\tilde{e}}_{w_r} \end{bmatrix} = \begin{bmatrix} 0 & I \\ -K_{ep_{iw_r}} & -K_{ep_{w_r}} \end{bmatrix} \begin{bmatrix} \tilde{e}_{iw_r} \\ \tilde{e}_{w_r} \end{bmatrix} + \begin{bmatrix} -\hat{\sigma}_{\nu_r} \\ \hat{\sigma}_r - \sigma_r \end{bmatrix}$$

The uncertainty estimates for inner loop can be computed as follows

$$\begin{bmatrix} -\hat{\sigma}_{\nu_r} \\ \hat{\sigma}_r \end{bmatrix} = \begin{bmatrix} I & 0 \\ 0 & I \end{bmatrix} \phi_r^{-1} \mu_r(iT_s)$$

where the parameters can be expressed as

$$\phi_r = -\begin{bmatrix} 0 & I \\ -K_{ep_{iw_r}} & -K_{ep_{w_r}} \end{bmatrix}^{-1} \left(\exp\left(\begin{bmatrix} 0 & I \\ -K_{ep_{iw_r}} & -K_{ep_{w_r}} \end{bmatrix} T_s \right) - I \right) \tag{32}$$

and

$$\mu_r(iT_s) = \exp\left(\begin{bmatrix} 0 & I \\ -K_{ep_{iw_r}} & -K_{ep_{w_r}} \end{bmatrix} T_s \right) \begin{bmatrix} \tilde{e}_{iw_r}(iT_s) \\ \tilde{e}_{w_r}(iT_s) \end{bmatrix}$$

4.2 Outer Loop L_1 Adaptive Control Design

L_1 Adaptive augmentation for outer Loop is designed as follows. The outer loop uncertainties are estimated and control laws are designed to nullify the effect of disturbances Peter et al. (2012).

The Eq.(1) to Eq.(3) can be re written as follows

$$\dot{Z}_{ro} = \hat{A}_{ro}(\wedge_{ro} \omega_{ro} + f_{ro}) + \hat{B}_{ro} \tag{33}$$

Where, the terms are defined as

$$\hat{A}_{ro} = \begin{bmatrix} -\bar{q}S/m & 0 & 0 \\ 0 & \bar{q}S/m & 0 \\ 0 & 0 & -\bar{q}S/m \end{bmatrix}, \quad f_{ro} = \begin{bmatrix} x_0 + C_{x_\alpha} + C_{x_{\delta_e}} \delta_e \\ C_{y_\beta}\beta + C_{y_{\delta_a}} \delta_a + C_{y_{\delta_r}} \delta_r \\ z_0 + C_{z_\alpha} + C_{z_\beta}\beta + C_{z_{\delta_e}} \delta_e \end{bmatrix}$$

$$\wedge_{ro} = \begin{bmatrix} 0 & C_{x_q}(c/2V_T) & 0 \\ C_{y_p}(b/2V_T) & 0 & C_{y_r}(b/2V_T) \\ 0 & C_{z_q}(c/2V_T) & 0 \end{bmatrix} \tag{34}$$

$$\omega_{ro} = \begin{bmatrix} P \\ Q \\ R \end{bmatrix}, \ \hat{B}_{ro} = \begin{bmatrix} X_t - g\sin\theta + RV - QW \\ g\cos\phi\cos\theta + QU - PV \\ g\sin\phi\cos\theta + PW - RU \end{bmatrix}$$

In order to design the outer loop state predictor, the plant dynamics in L_1 framework is provided as

$$\dot{Z}_{ro} = \hat{A}_{ro}\omega_{ro} + \hat{B}_{ro} + \sigma_{ro}, \quad \sigma_{ro} = \hat{A}_{ro}[(\wedge_{ro} - I)\omega_{ro} + f_{ro}] \tag{35}$$

Where, σ_{ro} is Composite Uncertainty and it estimates the uncertainties in the approximate model represented by $\hat{A}_{ro}$ and $\hat{B}_{ro}$.

Piece Wise Constant Adaptive Laws: Predictor equation for the outer loop is provided as follows

$$\dot{\hat{Z}}_{ro} = \hat{A}_{ro}\omega_{ro} + \hat{B}_{ro} + \hat{\sigma}_{ro} - K_{ep_{w_{ro}}} \tilde{e}_{w_{ro}} \tag{36}$$

$$\tilde{e}_{w_{ro}} = \hat{Z}_{ro} - Z_{ro} \tag{37}$$

$$\dot{\tilde{e}}_{w_{ro}} = \hat{\sigma}_{ro} - \sigma_{ro} - K_{ep_{w_{ro}}} \tilde{e}_{w_{ro}} \tag{38}$$

Outer loop piece wise constant adaptation laws are given as follows

$$\hat{\sigma}_{ro}(t) = -\phi_{ro}^{-1} \mu_{ro}(iT_s) \quad t \in [iT_s, (i+1)T_s) \tag{39}$$

$$\phi_{ro} = (-K_{ep_{w_{ro}}})^{-1}(e^{-K_{ep_{w_{ro}}} T_s} - I) \tag{40}$$

$$\mu_{ro}(iT_s) = e^{-K_{ep_{w_{ro}}} T_s} \tilde{e}_{w_{ro}}(iT_s) \tag{41}$$

Outer loop adaptive control is provided as

$$\omega_{ado} = C_{ro}(s)(\hat{A}_{ro})^{-1}[-\hat{\sigma}_{ro}] \tag{42}$$

Inner loop adaptive control is provided as Shivendra N Tiwari and Padhi (2016)

$$\nu_{ad} = C_r(s)(\hat{A}_r)^{-1} \left[-\hat{\sigma}_r + K_p \omega_{ado} + K_I \int \omega_{ado}\, dt + \dot{\omega}_{ado} \right] \tag{43}$$

Total Control computed for the plant is addition of baseline NDI controller and L_1 adaptive controller.

$$\nu = \nu_{bl} + \nu_{ad} \tag{44}$$

5. SIMULATION RESULTS

This section presents the results for auto landing of a UAV with Six-DOF model. The low pass filters are designed for each case as well as the adaptive gains are also set based on problem requirement. The UAV autonomous landing trajectory is shown in Fig. 3. During the glide-slope path, the UAV follows the -3^0 ramp trajectory. Once the decision height is obtained the exponential flare trajectory is tracked. The Six-DOF plant is perturbed with wind shear, wind gust and ground effects, initial position of the UAV is set as $[-1500, 20, 50]$. The Fig. 3 shows performance of NDI controller for a nominal plant, NDI controller for plant with uncertainties, NDI augmented with L_1 adaptive controller for plant with uncertainties. It can be seen in the Fig. 3 that when UAV approaches ground, the ground effect comes into existence at around twice the wingspan($b = 2m$) altitude. The NDI autopilot is not able to track the desired

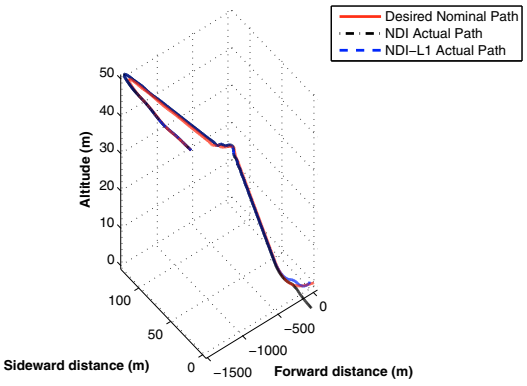

Fig. 3. UAV Trajectory

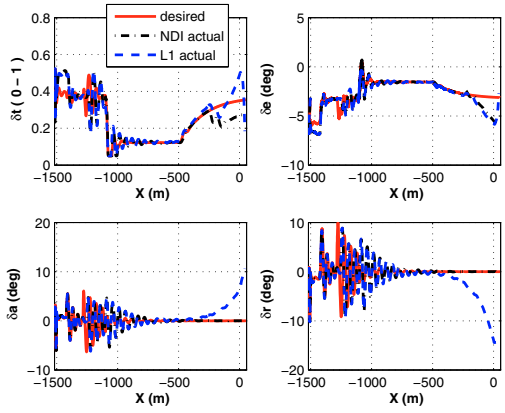

Fig. 4. UAV Total Control Commands

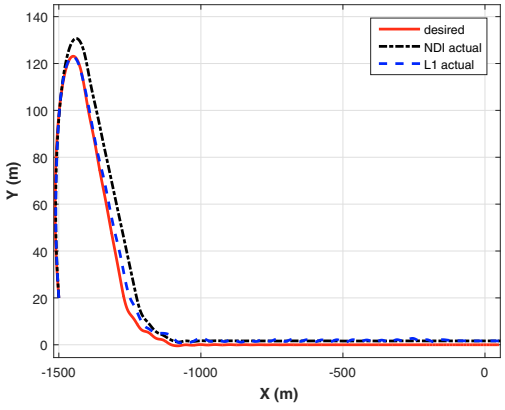

Fig. 5. UAV Landing Trajectory XY Plane View

trajectory. However, NDI autopilot augmented with L_1 adaptive controller tracks the desired trajectory.

Total Control commands of UAV are shown in Fig. 4. The cross wind introduced in the plant is $1m/s$ along with ground effect active at around $3m$ altitude onwards.

The other simulation is shown in Fig. 5. The wind shear introduced is $[1.0, 0.8, 0.6]$ as well as wind gust $1m/s$ at 20 feet. The performance of L_1 adaptive control augmented with NDI command plots are shown with respect to NDI controls. NDI is not able to follow the desired track. The simulation results show that under plant perturbation and external disturbances, NDI augmented with L_1 adaptive controller performs fast adaptation for uncertainties and tracks the reference trajectory closely.

6. CONCLUSIONS

The autonomous landing problem for a UAV with Six-DOF model has been attempted using NDI controller with L_1 adaptive controller augmentation. In this paper, autonomous landing problem is attempted in presence of wind shear, wind gust and ground effects. NDI controller is controlling the nominal model of the UAV and L_1 adaptive controller augmentation is used to provide the correction in control to deal with uncertainties. During the glideslope mode, UAV tracks the constant flight path angle and during the flare mode it tracks the exponential trajectory with fixed sink rate at the touchdown point. Trim state of the UAV is used as initial state. Pitch, roll and yaw angles were controlled in order to keep the UAV on track. Velocity control was also implemented to keep the velocity constant during the landing process. NDI augmented with L_1 adaptive control algorithm converges faster and provides accurate tracking even in presence of disturbances and uncertainties.

REFERENCES

Anderson, J.D. (2007). *Introduction to Flight*. Tata McGraw Hill Education Private Limited, New Delhi, 5th edison edition.

Chawla, C. and Padhi, R. (2011). Integrated guidance and control of uavs for reactive collision avoidance. Technical report, DTIC Document.

Etkin, B. (2012). *Dynamics of atmospheric flight*. Courier Corporation.

Frost, W. and Bowles, R.L. (1984). Wind shear terms in the equations of aircraft motion. *Journal of Aircraft*, 21(11), 866–872.

Hovakimyan, N. and Cao, C. (2010). *L1 adaptive control theory: guaranteed robustness with fast adaptation*, volume 21. Siam.

Peter, F., Holzapfel, F., Xargay, E., and Hovakimyan, N. (2012). L1 adaptive augmentation of a missile autopilot. In *Proceedings of the AIAA Guidance, Navigation, and Control Conference*.

Prasad, B. and Pradeep, S. (2007). Automatic landing system design using feedback linearization method. In *AIAA Conference and Exhibit,7-10 May, Rohnert Park, California*, ,7-10 May,. AIAA Conference and Exhibit, ,7-10 May, Rohnert Park, California.

Shivendra N Tiwari, P N Dwivedi, A.B. and Padhi, R. (2016). L1 adaptive nonlinear dynamic inversion missile autopilot with pi structure and adaptive sampling. In *Indian Control Conference*.

Singh, S. and Padhi, R. (2009). Automatic path planning and control design for autonomous landing of uavs using dynamic inversion. In *2009 American Control Conference*, 2409–2414. IEEE.

Stevens, B.L., Lewis, F.L., and Johnson, E.N. (2015). *Aircraft Control and Simulation: Dynamics, Controls Design, and Autonomous Systems*. John Wiley & Sons.

Wagner, T. and Valasek, J. (2007). Digital autoland control laws using quantitative feedback theory and direct digital design. *Journal of Guidance, Control, and Dynamics*, 30(5), 1399–1413.